Bulk Synthesis of Inorganic Fullerene-like MS_2 (M = Mo, W) from the Respective Trioxides and the Reaction Mechanism

Y. Feldman,[†] G. L. Frey,[†] M. Homyonfer,[†] V. Lyakhovitskaya,[†] L. Margulis,[†,‡] H. Cohen,[‡] G. Hodes,*[,†] J. L. Hutchison,[§] and R. Tenne*[,†]

Contribution from the Department of Materials and Interfaces, Weizmann Institute, Rehovot 76100, Israel, Department of Chemical Services, Weizmann Institute, Rehovot 76100, Israel, and Department of Materials, University of Oxford, Parks Road, Oxford OX1 3PH, U.K.

Received January 23, 1996[⊗]

Abstract: Recently, milligram quantities of MoS_2 fullerene-like nanotubes and negative curvature polyhedra (generically called *inorganic fullerene-like material, IF*), were reproducibly obtained by a gas phase reaction from an oxide precursor (Feldman, Y.; Wasserman, E.; Srolovitz, D. J.; Tenne, R. *Science* **1995**, *267*, 222. Srolovitz, D. J.; Safran, S. A.; Homyonfer, M.; Tenne, R. *Phys. Rev. Lett.* **1995**, *74*, 1778). The present work focuses on the mechanism of the synthesis of IF-MS_2 (M = W, Mo). The IF material is obtained from oxide particles smaller than ca. 0.2 μm, while larger oxide particles result in 2H-MS_2 platelets. The key step in the reaction mechanism is the formation of a closed layer of MS_2, which isolates the nanoparticle from its surroundings and prevents its fusion into larger particles. Subsequently, the oxide core of the nanoparticle is progressively converted into a sulfide nanoparticle with an empty core (IF). Taking advantage of this process, we report here a routine for the fabrication of macroscopic quantities of a pure IF-WS_2 phase with a very high yield. As anticipated, the size distribution of the IF material is determined by the size distribution of the oxide precursor. The present synthesis paves the way for a systematic study of these materials which are promising candidates for, e.g., solid lubrication.

Introduction

Notwithstanding the efforts to develop synthetic routes for the mass production of carbon fullerenes, nested fullerenes ("buckeyonions"), nanotubes, etc., the generic technique for the synthesis of such phases remains arc-discharge[3,4] and subsequent extraction from the soot. A similar process is also used for the synthesis of BN or $B_xC_yN_x$ nanotubes,[5,6] metallocarbohedrenes (Met-Cars),[7] endohedral fullerenes,[8] and nanotubes.[9] Obviously, this method is neither very easy to control nor amenable to an easy scale-up. The ensuing purification processes are tedious and time consuming, which influences the cost of the final product. Key steps in the growth mechanism of these products were elucidated,[10,11] but the detailed mechanism of the reaction is still a matter of controversy. Therefore, the size distribution of nanotubes and nested fullerenes cannot be adequately controlled and is relatively wide. For both species, the innermost layer serves as a template for the growth of the top layers, which usually grow outward,[11−13] possibly in an accretion (snail-like) growth mode.[14] The synthesis of inorganic MX_2 (M = W, Mo; X = S, Se) nested fullerene-like structures and nanotubes has been described recently.[15] This study demonstrated that the propensity to form polyhedral structure is not unique to carbon, but is likely to be commonplace among nanoparticles of 2-D layered compounds.[16] Subsequently, a gas phase synthesis of molybdenum trioxide precursor was used to obtain a few milligrams of IF-MoS_2 (IF = inorganic fullerene-like material).[1,2] In contrast to the synthesis of carbon-nested fullerenes, the present process lends itself for an easy scale-up using low-cost feedstocks, and therefore relatively inexpensive products could be foreseen.

In this paper we present a model for the growth mechanism of the IF-MS_2 phase from an oxide precursor. Although the syntheses of the IF phases of MoS_2 and WS_2 differ in some important details, the salient features are common to both products. A schematic representation of the growth mode of an IF particle is depicted in Figure 1. Within the first few seconds of the reaction, the top surface of the oxide nanoparticle reacts with H_2S gas and a completely closed monomolecular MS_2 layer or two are formed. Similar behavior of oxide nanoparticles in H_2S atmosphere has been inadvertently ob-

[†] Department of Materials and Interfaces, Weizmann Institute.
[‡] Department of Chemical Services, Weizmann Institute.
[§] University of Oxford.
[⊗] Abstract published in *Advance ACS Abstracts,* May 15, 1996.

(1) Feldman, Y.; Wasserman, E.; Srolovitz, D. J.; Tenne, R. *Science* **1995**, *267*, 222.
(2) Srolovitz, D. J.; Safran, S. A.; Homyonfer, M.; Tenne, R. *Phys. Rev. Lett.* **1995**, *74*, 1778.
(3) Krätschmer, W. A.; Lamb, L. D.; Fostiropoulos, K.; Huffman, D. R. *Nature* **1990**, *347*, 354.
(4) Ebbesen, T. W.; Ajayan, P. M. *Nature* **1992**, *358*, 220.
(5) Stephane, O.; Ajayan, P. M.; Colliex, C.; Redlich, Ph.; Lambert, J. M.; Bernier, P.; Lefin, P. *Science* **1994**, *266*, 1683.
(6) Weng-Sieh, Z.; Cherrey, K.; Chopra, N. G.; Blase, X.; Miyamoto, Y.; Rubio, A.; Cohen, M. L.; Louie, S. G.; Zettl, A.; Gronsky, R. *Phys. Rev. B* **1994**, *51*, 11229.
(7) Cartier, S. F.; Chen, Z. Y.; Walder, G. J.; Sleppy, C. R.; Castleman, A. W. *Science* **1995**, *260*, 195.
(8) (a) Chai, Y.; Guo, T.; Jin, C.; Haufler, R. E.; Chibante, L. P. F.; Fure, J.; Wang, L.; Alford,J. M.; Smalley, R. E. *J. Phys. Chem.* **1991**, 95, 7564. (b) Takata, M.; Umeda, B.; Nishibori, E.; Sakata, M.; Saito, Y.; Ohno, M.; Shinohara, H. *Nature* **1995**, *377*, 46.
(9) (a) Ruoff, R. S.; Lorents, D. C.; Chan, B.; Malhorta, R.; Subramoney, S. *Science* **1993**, *259*, 346. (b) Tomita, M.; Saito, Y.; Hayashi, T. *Jpn. J. Appl. Phys.* **1993**, *32*, L280. (c) Seraphin, S.; Zhou, D.; Jiao, J.; Withers, J. C.; Lotfy, R. *Nature* **1993**, *362*, 503. (d) Yosida, Y. *Appl. Phys. Lett.* **1993**, *62*, 3447.
(10) Jarrold, M. J.; et al. *J. Phys. Chem.* **1994**, *98*, 1810.
(11) (a) Iijima, S. *Mater. Sci. Eng.* **1993**, *B19*, 172. (b) Iijima, S.; Ajayan, P. M.; Ichihashi, T. *Phys. Rev. Lett.* **1992**, *69*, 3100.
(12) Ugarte, D. *Nature* **1992**, *359*, 707.
(13) (a) Ugarte, D. *Chem. Phys. Lett.* **1992**, *198*, 596. (b) Ugarte, D. *Z. Phys. D: At., Mol. Clusters* **1993**, *26*, 150. (c) Ugarte, D. *Europhys. Lett.* **1993**, *22*, 45.
(14) Kroto, H. W. *Science* **1988**, *242*, 1139.
(15) (a) Tenne, R.; Margulis, L.; Genut, M.; Hodes, G. *Nature* **1992**, *360*, 444. (b) Margulis, L.; Salitra, G.; Tenne, R.; Talianker, M. *Nature* **1993**, *365*, 113. (c) Hershfinkel, M.; Gheber, L. A.; Volterra, V.; Hutchison, J. L.; Margulis, L.; Tenne, R. *J. Am. Chem. Soc.* **1994**, *116*, 1914.
(16) Choppra, N. G.; Luyken, R. J.; Cherrey, K.; Crespi, V. H.; Cohen, M. L.; Louie, S. G.; Zettl, A. *Science* **1995**, *269*, 966.

S0002-7863(96)00240-5 CCC: $12.00

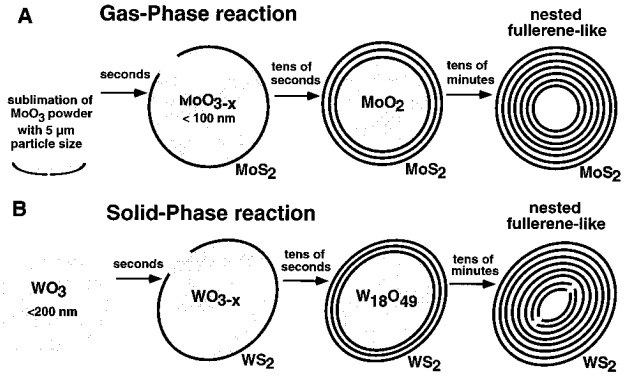

Figure 1. Schematic representation of the growth model of the inorganic fullerene-like phase of MoS_2 (A) and WS_2 (B) nested polyhedra from oxide nanoparticles.

served before.[17] The inert surface−sulfide layer prohibits fusion of nanoparticles into macroscopic entities, which would lead to the formation of the 2H-MS_2 phase. Fast hydrogen diffusion into the nanoparticle leads to a complete reduction of the oxide core into MoO_2 or $W_{18}O_{49}$, within a minute or two.[18] Subsequently, the oxide core is progressively converted into the respective sulfide (IF) through a slow diffusion-controlled reaction, which ends after ca. 30 min. Consequently, *the size of the IF particle is determined by the size of the incipient oxide nanoparticle*.

Experimental Section

Molybdenum oxide is volatile under reducing conditions above 700°C, and hence a gas phase reaction was adopted for the synthesis of IF-MoS_2.[19] A detailed account of the gas phase reaction for the synthesis of IF-MoS_2 has been reported previously[1,2] and will be repeated only briefly here. Typically a portion of 30 mg of MoO_3 powder (>99% pure) is heated (>800 °C) and is slowly reduced to MoO_{3-x} by a stream of forming gas (typically 5%H_2/95%N_2).[20] The suboxide sublimes and effuses out of a nozzle where it crosses a stream of H_2S gas mixed with a forming gas. It takes 3−5 min. for the entire load of MoO_3 to sublime. The reaction products are collected on a quartz substrate, which is positioned 3 cm away from the crossing point of the two gas streams and is maintained at the same temperature (>800 °C). The collected nanoparticles are progressively converted into nested IF polyhedra within ca. 30 min of firing time. The average size of the oxide nanoparticle and the ensuing IF-MoS_2 increases with temperature. It was found that above 900 °C, platelets with 2H-MoS_2 structure abound, and become the sole product above 950 °C.

Since WO_3 is not volatile at these temperatures, the solid (WO_3)−gas (H_2S + H_2) reaction was preferred, in this case.[15a] The starting material for the synthesis of IF-WS_2 is a WO_3 powder (>99% pure), with particle sizes smaller than ca. 150 nm. To avoid agglomeration and fusion of the heated nanoparticles, the powder was carefully dispersed on the entire floor of the reactor boat, resulting in a complete exposure of the nanoparticle surface to the reacting gas. 2H-WS_2 platelets were predominantly obtained under the following experimental conditions: packing of the powder was too compact; oxide particles with sizes above 0.2 μm were used; the reaction temperature exceeded 900 °C.

Complementary information on the reaction mechanism was obtained by using a combination of the following techniques: transmission electron microscopy (TEM), electron diffraction (ED), X-ray powder diffraction (XRD), X-ray photoelectron spectroscopy (XPS), and optical absorption measurements.

Results and Discussion

Figure 2 shows a series of TEM images demonstrating the progression of the conversion of MoO_2 particles into IF-MoS_2 (A−D). Since, the sublimation of the MoO_3 powder is not instantaneous, the extent of oxide to sulfide conversion of the nanoparticles is not uniform, particularly at the early stages of the process. Therefore, the number of MoS_2 layers varies from point to point on the quartz collector. Parts A−C of Figure 2 exhibit a series of stages in the conversion of a typical sample, which was retracted from the oven after 5 min. Figure 2A shows a number of MoO_2 particles covered by two to three closed layers of MoS_2. Particles covered with four layers of MoS_2, which were collected at another location of the quartz slide, are displayed in Figure 2B. Figure 2C shows a particle with at least six closed layers of MoS_2. Electron diffraction (inset) confirmed that the inner core of the IF consists of MoO_2.[21] Most remarkably, a growth front of eight layers, which is seldom observed, is advancing into the oxide core on the upper-right side of the IF. The intermediate zone between the crystalline MoO_2 core and the advancing front of IF-MoS_2 appears structureless and is likely to consist of a disordered molybdenum oxysulfide.[22] An assortment of completely converted IF-MoS_2 particles is shown in Figure 2D, and is typically obtained after 30 min of reaction time at 850 °C. The growth mechanism can be regarded in terms of a substitution model which is the opposite of the accretion model proposed previously for carbon fullerenes.[14] The size of the MoO_{3-x} nanoparticles, which sublime from the MoO_3 source and are deposited on the quartz collector, increases with the temperature from 10 nm at 820 °C to 100 nm and above at 870 °C.[1] Therefore, the size of an IF particle is fully determined by the size of the incipient oxide nanoparticle which serves as its precursor. It is noticed that, while the particles exhibit a more spherical-like morphology in the beginning of the sulfidization process (Figure 2A,B), they show faceted morphology, with casps and well-defined angles at the end of the process (Figure 2D). Moreover, the outer layers which are obtained in the initial stages of the sulfidization process remain mostly unchanged at the end of the process (Figure 2D), while the innermost layers with a smaller diameter exhibit much more faceted morphology. Edge dislocations are being formed and observed between the two morphologies. A continuum model has recently been used to calculate the shape of nested fullerenes. This model predicted a phase transformation from structures with spherical shape into faceted ones as the thickness (number of layers) of the particles increases beyond a critical value or the radius of curvature decreases beyond a certain critical value.[2] This qualitative agreement between theory and experiment indicates that continuum models can provide useful guidelines for IF synthesis.

In the case of IF-WS_2, the precursor is solid WO_3, and hence the size of the oxide nanoparticles (Figure 2E,G) determines the size of the IF particles (Figure 2F,H). In contrast to the molybdenum case, the H_2S gas reacts uniformly with all oxide particles in the powder, and hence the number of sulfide layers is essentially the same for all intermediate IF-WS_2/oxide composite nanoparticles.

Figure 3 presents the XRD spectra of a WO_3 powder acquired during different stages of the annealing process. The XRD pattern of the precursor coincides with that of WO_3 (Figure 3A).

(17) Sanders, J. V. *J. Electron Microsc. Tech.* **1986**, *3*, 67.
(18) *Transition Metal Oxides*; Kung, H. H., Ed.; Amsterdam−Oxford−New York−Tokyo, 1989, Vol.45, p 93.
(19) Although the main route for the synthesis of IF-MoS_2 was through the gas phase reaction, a solid−gas reaction was used as well. The details of the reaction were very similar to those of IF-WS_2, but the yield was appreciably smaller due to sublimation of some of the oxide powder.
(20) The forming gas is necessary in order to reduce the more stable oxide and divert the reaction path to the sulfide products.
(21) Schmidt, E.; Weill, F.; Meunier, G.; Levasseur, A. *Thin Solid Films* **1995**, *260*, 21.
(22) Schmidt, E.; Sourisseau, C.; Meunier, G.; Levasseur, A. *Thin Solid Films* **1994**, *245*, 34.

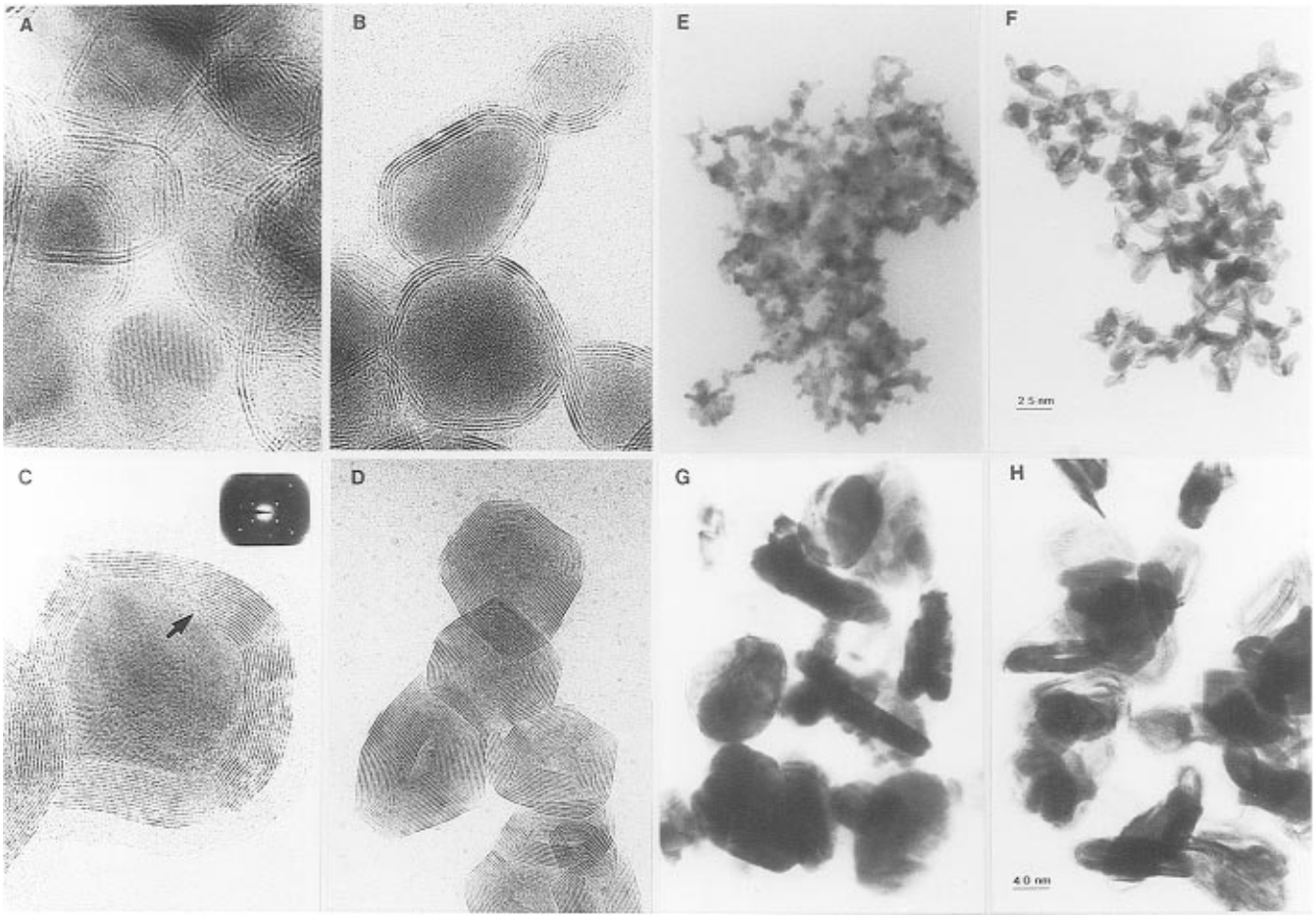

Figure 2. TEM micrographs showing the gradual transformation of molybdenum oxide nanoparticles into IF-MoS_2 (A−D) nested polyhedra. The electron diffraction pattern inset of (C) is consistent with (111) of MoO_2. (E) shows a typical assortment of tungsten oxide particles with <10 nm diameter which are transformed into IF-WS_2 particles of a similar size (Figure 2F). (G) and (H) show a similar transformation for tungsten oxide particles with a diameter in the range of 50−100 nm. Note that both oxide and IF phases contain very asymmetric particles. The interlayer spacing of 0.62 nm is clearly visible in (A)−(D).

After 2 min of annealing, a small WS_2 peak was observed (Figure 3B). Astonishingly, the entire nanoparticle core has been reduced to $W_{18}O_{49}$ at this early stage of the process. This fact can be understood assuming that hydrogen and water diffuse appreciably faster than sulfur diffuses to form sulfide. Figure 3C shows the state of the sample after 8 min of annealing, while Figure 3D displays the XRD patterns of the sample after 15 min of annealing time. The fully converted sample (120 min) is shown in Figure 3E. The shift of the (0002) peak of the IF-WS_2 phase (Figure 3D) indicates a lattice expansion of ca. 2% between two adjacent WS_2 slabs along the *c*-axis, which is attributed to the strain in the bent layers.[1] Furthermore, since the number of atoms in the layer increases with its radius, the layers cannot be fully commensurate. This discrepancy can be partially alleviated by lattice expansion along the *c*-axis. A similar study has been carried out for the conversion of MoO_2 into IF-MoS_2, the results being essentially the same as those shown in Figure 3.

Optical absorption spectra at different temperatures were measured for a sample consisting of IF-MoS_2 (shell)/MoO_2 (core) particles at different annealing times, including a pure IF-MoS_2 film (Figure 4A). A reference 2H-MoS_2 crystal was measured as well. Comparison of the spectra of IF-MoS_2 to that of the (2H) bulk phase at the same temperature reveals a red shift in the excitonic absorption of the former. The A, B, and C excitons appear at 667, 616.3, and 525 nm, respectively, in the IF phase at 175 K, while their energies in the 2H phase are 654.3, 593.5, and 490 nm.[23,24] After 3 min of annealing time of the oxide, the A and B excitons of the sulfide are already noticeable. The C exciton partially overlaps with the dominant absorption of MoO_2 at 500 nm.[25] The intensity of the oxide absorption decreased, while the exciton absorption increased with annealing time. After 90 min of annealing time, the exciton absorption peaks of the sulfide increased by a factor of 2.5 compared with the 3 min annealed sample. The oxide absorption disappeared completely. The transformation of WO_{3-x} into IF-WS_2 (Figure 4B) was followed by using stirred alcoholic suspensions at room temperature. The oxide absorption peak of the composite oxide/sulfide (6 min annealing time) could be easily resolved in the difference spectrum and is substantially red shifted, compared to the literature value.[25] Remarkably, IF-MS_2 powder consisting of particles smaller than 10 nm formed a stable alcoholic colloid exhibiting a strong blue shift of the excitonic absorption, which could be possibly assigned to a quantum size effect.[24]

Being a surface sensitive technique, XPS could be ideally suited for investigating the sulfide/oxide superstructure. Accordingly, a few milligrams of IF-WS_2 powder, synthesized by the solid−gas reaction, was pressed onto an indium plate, which provided the support and electrical contact for the powder. A

(23) Wilson, J. A.; Yoffe, A. D. *Adv. Phys.* **1968**, *18*, 193.
(24) Frey, G. L.; Homyonfer, M.; Feldman, Y.; Tenne, R. To be published.
(25) Porter, V. R.; White, W. B.; Roy, R. *J. Solid State Chem.* **1969**, *1*, 359.

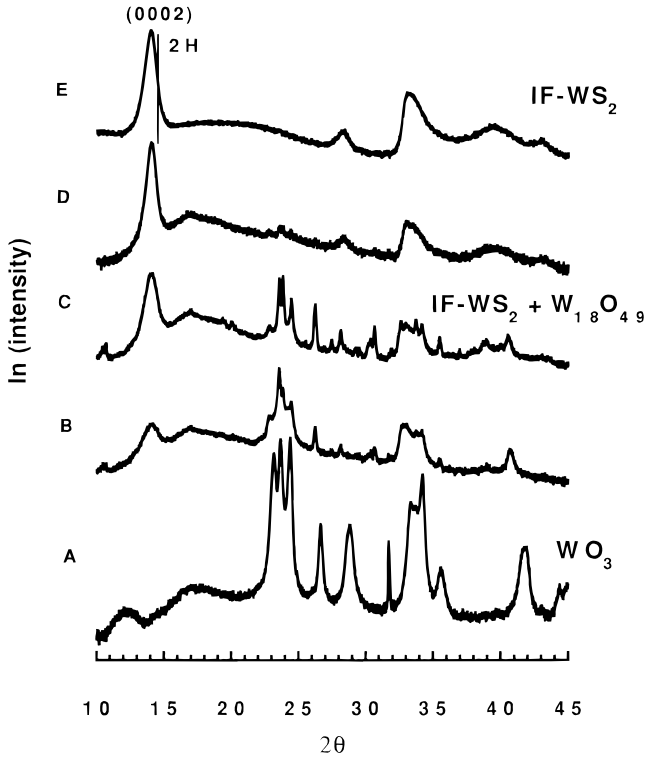

Figure 3. Transformation of WO_3 nanoparticles into IF-WS_2 followed by X-ray powder diffraction: (A) WO_3 precursor; (B) the same powder after 2 min of annealing; (C) after 8 min of annealing; (D) 15 min of annealing. Annealing conditions: 850 °C; rates of gas flow, forming gas, 130 cm^3/min; H_2S, 2 cm^3/min.

sequence of four samples consisting of composite nanoparticles of IF-WS_2 (shell)/tungsten oxide (core) at different annealing times at 850 °C were investigated: sample 1, 2 min; 2, 6 min, 3, 15 min; 4, 2 h. In addition, reference WS_2 crystal, WO_3 powder, and a clean indium specimen were measured. The fraction of oxide particle converted into sulfide was determined in two independent ways, which gave similar results. The concentration of the two compounds was determined first from the analysis of the total concentrations of the various elements, and second from the tungsten 4f−5p spectral region which was deconvoluted into sulfide ($4f_{7/2}$, 32.6; $4f_{5/2}$, 34.75; $5p_{3/2}$, 38.3 eV) and oxide (shifted to higher energies by 3.0 eV). Shirley background subtraction was used for spectral analysis.[26] While the indium contribution to the total signal was less than 1%, carbon made up to 18% of the total material. Yet, by comparing the molybdenum and sulfur line shapes with those of pure 2H-MoS_2, it was concluded that the carbon was not incorporated in the fullerene-like nanoparticles. The source of carbon contamination is likely to originate from adsorbed organic molecules having a mean thickness of 4−7 Å. Such an adsorbant signal does not seriously influence the analysis of its support, the fullerene-like material. Removal of the carbon contamination by ion sputtering was harmful to the IF structures and is not presented. Additional confirmation of that point came from local (TEM) electron energy loss measurements, which proved (due to its low sensitivity to surface contamination) that each nanoparticle consisted exclusively of Mo and S.

The spectra of 2H-WS_2 crystal and oxide powder, with line broadening permitted, were used as model line shapes for the deconvolution. The total error in this calculation was estimated at 1%. The high reliability of the deconvolution procedure was reaffirmed by using different pass energies. The results,

(26) *Practical Surface Analysis*, 2nd ed.; Briggs, D., Seah, M. P., Eds.; John Wiley & Sons: New York, 1990, Vol. 1, p 233.

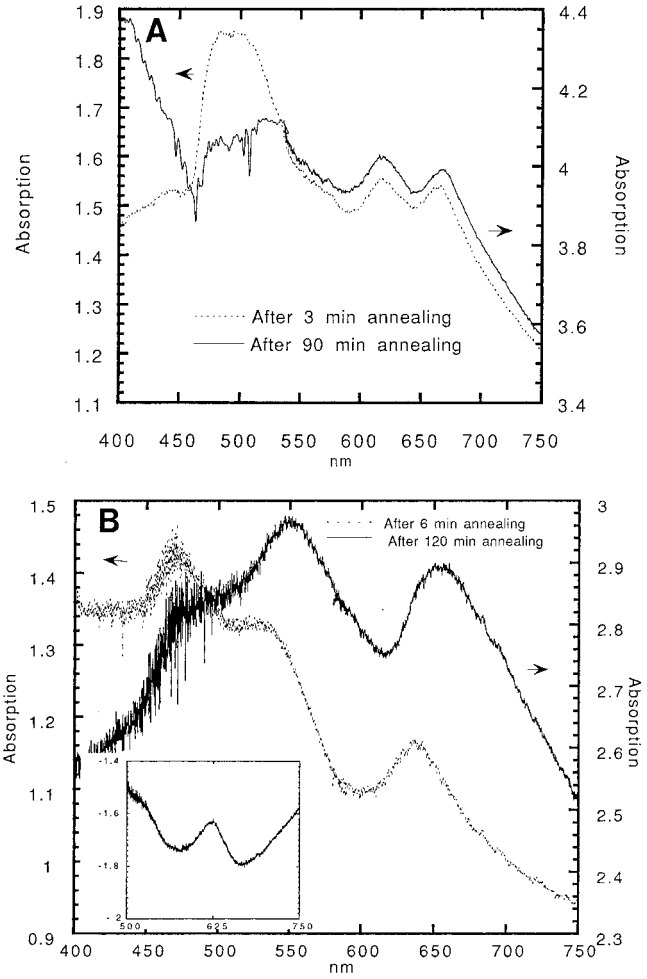

Figure 4. Optical absorption measurements of (A) a composite IF-MoS_2/MoO_2 sample obtained through the gas phase reaction and accrued on a quartz substrate after 3 min of annealing (dashed line) and after prolonged (90 min) annealing (solid line) and (B) a composite IF-WS_2/WO_{3-x} sample after 6 min of annealing (dashed line) and after 120 min of annealing (solid line). The inset shows the difference spectra (oxide absorption peak). Annealing conditions are as in Figure 3.

Table 1. Conversion of Tungsten Oxide into IF-WS_2, Obtained from the Deconvolution of the W (4f) Peaks in a Series of XPS Spectra[a]

annealing time (min)	I_{ox} (%)	I_{sul} (%)	d/λ	k
2	38	62	0.6	2
6	11	89	1.5	5
15	1.5	98.5	3.3	11
120	<0.5	>99.5		

[a] Monochromatized Al Kα ($h\nu$ = 1486.6 eV) was used for the excitation. A monchromatized beam (0.7 eV resolution) and a base pressure of 10^{-9} Torr were used.

expressed as I_{sul} and I_{ox}, are summarized in Table 1. The relative intensities I_{sul}/I_{ox} can be converted into sulfide shell thickness (d) or number of dichalcogenide layers (k) by considering a model type polyhedron, for which the shell and core intensities are calculated face by face:

$$I_{sul}/I_{ox} = \sum W_n I_{n,sul} / \sum W_n I_{n,ox} \qquad (1)$$

where W_n is the projection of the face area on the plane normal to the electron take-off direction (that is, parallel to the substrate plane). For simplicity we choose a regular polyhedron for the

Table 2. Kinetics of the Reduction of WO_3 Nanoparticles into Suboxides and its Conversion into IF-WS_2 Studied by XRD for Samples Prepared under Different Experimental Conditions

gas atmosphere; flow rate (cm^3/ min)	av size of oxide particles(μm)	temp (°C)	reactn time (h)	product of reactn (XRD)	av particle size (μm) (TEM)
H_2S; 4.5 + H_2(5%)/N_2; 100	3−5	500	3	WO_3	not changed
		640	1	$WS_2 + W_{20}O_{58}$	0.1−3
		820	1	$WS_2 + W_{20}O_{58} + W_{18}O_{49}$	
		870	2	2H-$WS_2 + W_{18}O_{49}$	2−10
		970	1	2H-$WS_2 + WO_2 + W_{18}O_{49}$	
	∼0.1	150	18	WO_3	not changed
		300	9	WS_2/WO_3	
		400	4	$WS_2/W_{20}O_{58}$	
		700	0.3	IF-$WS_2/W_{20}O_{58}$	
		820	0.3	IF-$WS_2/W_{18}O_{49}$	
		820	2	IF-WS_2	
		870	2	IF-WS_2 + 2H-$WS_2 + W_{18}O_{49}$	2−10
		970	1	2H-$WS_2 + W_{18}O_{49} + WO_2$	
H_2(5%)/N_2; 100	∼0.1	560	2	WO_3	not changed
		570	1.5	$W_{20}O_{58}$	
		600	1	$W_{20}O_{58} + W + W_{18}O_{49}$	0.06−0.1
		650	1.5	$WO_2 + W$	0.03−0.1
		770	0.2	$W_{18}O_{49}$	0.1−1
		820	0.3	$W_{18}O_{49}$	1−2
		970	0.3	$WO_2 + W$	1−6
	3−5	630	1	WO_3	not changed
		650	1.5	$WO_3 + WO_2$	0.1−3
		750	0.2	$W_{20}O_{58}$	
		970	0.3	WO_2	1−6
H_2(1%)/N_2; 100	∼0.1	600	1.5	WO_3	not changed

analysis. The two I_n terms in eq 1 are given by[27]

$$I_{n,\mathrm{sul}} = \int_0^{d/\cos\theta_n} \mathrm{d}z\, I_{0(\mathrm{sul})} \exp(-z/\lambda \cos\theta_n) + \int_{D_n+d/\cos\theta_n}^{D_n+2d/\cos\theta_n} \mathrm{d}z\, I_{0(\mathrm{sul})} \exp(-z/\lambda \cos\theta_n)$$

$$I_{n,\mathrm{ox}} = \int_{d/\cos\theta_n}^{D_n+d/\cos\theta_n} \mathrm{d}z\, I_{0(\mathrm{ox})} \exp(-z/\lambda \cos\theta_n) \qquad (2)$$

The two terms in $I_{n,\mathrm{sul}}$ stand for the contributions from the top and bottom shells of the nth segment (slope). I_0 is a factor proportional to the partial density of tungsten in the compound: $I_{0(\mathrm{sul})} = I_0/3$; $I_{0(\mathrm{ox})} = I_0/3.7$. D_n is the thickness of the oxide under the face of segment n. λ is the escape depth of the photoelectrons.

The calculated values for d/λ and k, which are given in Table 1, were obtained for a polyhedron having only six different slopes (segments): $\theta_n = 15°n$, $n = 0, ..., N-1$. The number of slopes, $N = 6$, is a representative value. In fact the numerical result becomes only weakly dependent on N for $N > 3$. A similar model for spherical particles ($N \rightarrow \infty$) was recently published.[28] The value of λ was taken as ∼2 nm[29] and that of the interlayer distance as ∼0.62 nm.[23] The results of this analysis are in good agreement with the TEM observations; the main error stems from the variation in the number of MS_2 layers in the various nested polyhedra. XPS analysis of the MoO_2 into IF-MoS_2 conversion has been performed as well. Although the results of the analysis were qualitative in nature, the same trends as for the tungsten compounds have been observed.

The kinetics of the tungsten oxide reduction/sulfidization process was inferred from XRD measurements, and some typical results are presented in Table 2. From this table it is clear that, in addition to the experimental parameters, the size of the oxide particles plays an important role in the reduction/sulfidization reaction. For large (3−5 μm) particles, the reduction to the suboxide $W_{20}O_{58}$ and the subsequent sulfidization into WS_2 occur between 570 and 650 °C, whereas a powder consisting of small (0.1 μm) trioxide particles reacts at 400 °C. Furthermore, whereas the sulfidization of small particles occurs in a mode which leads to fullerene formation, the large particles form turbostratic-like WS_2 particles at temperatures lower than 600 °C, and 2H-WS_2 platelets upon sulfidization at elevated temperatures. In the absence of H_2S in the reactor, the reduction process is incomplete, and hence, it can be concluded that this gas serves as an auxiliary reducer of the oxide. Finally, the lower the concentration of hydrogen in the forming gas mixture, the slower was the reaction and the higher was the temperature required for the reaction. These considerations permit one to fine-tune the reaction conditions to the point that the IF-MS_2 phase can be synthesized with a very good reproducibility and yield.

Having the details of the reaction mechanism in mind, a modified reactor for the synthesis of macroscopic quantities of IF-WS_2 was constructed. The cross section of this reactor is illustrated schematically in Figure 5. To increase the amount of the (oxide) reactant and expose its entire surface to the gas, a bundle of tubes 7 mm in diameter each was placed inside the main tube (40 mm diameter) and the oxide powder was dispersed in them, very loosely. Typically, 1 g of IF-WS_2 could be obtained in a single batch, with a conversion yield of almost 100%.[30] This is remarkable in so far as the yield of production of carbon-nested fullerenes (and nanotubes) by the arc-discharge method is a few percent only.

In postulating a likely mechanism, we bear in mind the following: First, the reduction by H_2 is fast; the lower oxide is formed. Second, the formation of a thin sulfide skin controls the size of the fullerene. Since the size is thus fixed, the further transformation to sulfide must then take place internally.

A radial diffusion inward of the reactant (H_2S) and a similar diffusion outward of the product (H_2O) through the nanoparticle walls would appear unlikely in this case. Also, the large differences in time scales for the oxide reduction and the

(27) Reference 26, p 135.
(28) Sheng, E.; Sutherland, I. *Surf. Sci.* **1994**, *314*, 325.
(29) Reference 26, p 207.

(30) The major loss occurred from the evaporation of the oxide prior to the conversion with the first layer of the sulfide.

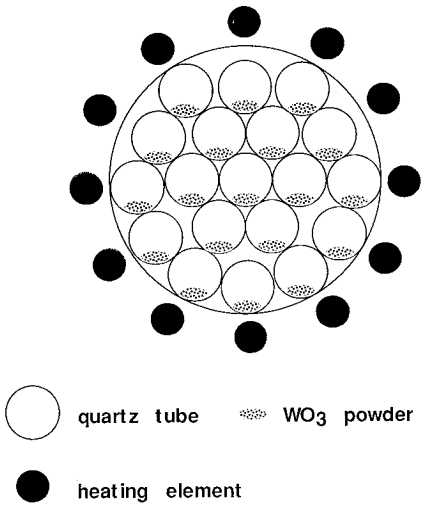

Figure 5. Cross section of the reactor which was used for the synthesis of bulk quantities of IF-WS_2.

subsequent sulfidization reaction suggest a different mechanism for the diffusion of hydrogen−oxygen and sulfur. It is hypothesized that the hydrogen and oxygen may diffuse through the layers (II*c*) radially, while sulfur atoms intercalate and diffuse easily along the MS_2 layers ($\perp c$) until they reach a dislocation or other fault which permits them to diffuse radially through the layer ($||c$) to the next inner layer. Such a mechanism would explain the fact that a single growth front is seen to advance *away* from structural defects at corners of the polyhedra (Figure 2C). The lattice expansion of ca. 20% of the *c*-axis, at the high temperature of the process (1100 K), facilitates the intercalation/diffusion of the reacting species.

Conclusions

Since the outer surface of the IF material exposes only the basal plane of the compound, this material lends itself to solid lubrication applications. Indeed, IF nanoparticles do not stick to each other or the substrate and exhibit poor surface adhesion. Their approximate spherosymmetric shapes imply easy sliding and rolling of the nanoparticles, and consequently very small shear forces are required to move them on the substrate surface. Preliminary results tend to support this hypothesis.[31] The oxide core (Figure 2C) provides the necessary mechanical toughness to the IF particle. Preliminary experiments indicate poor catalytic activity of the material, which is understandable, considering the surface termination by inert sulfur atoms. On the other hand, the potential of IF material for photocatalysis is promising due to the strong optical absorption, large surface area, and documented chemical inertness under illumination.[32]

Acknowledgment. This research was supported by the following agencies: US-Israel Binational Science Foundation, Petroleum Research Fund of the American Chemical Society, NEDO (Japan), Edith Reich Foundation of the Weizmann Institute, UK-Israel S&T Research Fund, and Israeli Ministry of Energy and Infrastructure (R&D branch).

JA9602408

(31) Rappoport, L.; Feldman, Y.; Homyonfer, M.; Cohen, S.; Tenne, R. To be published.

(32) Tributsch, H. *Structure and Bonding*; Springer Verlag: Berlin, 1982, Vol. 49, p 127.